IL-1 and TGF-β Modulation of Epithelial Basement Membrane Components Perlecan and Nidogen Production by Corneal Stromal Cells

Paramananda Saikia, Shanmugapriya Thangavadivel, Carla S. Medeiros, Luciana Lassance, Rodrigo Carlos de Oliveira, and Steven E. Wilson

Cole Eye Institute, Cleveland Clinic, Cleveland, Ohio, United States

Correspondence: Steven E. Wilson, Cole Eye Institute, I-32, Cleveland Clinic, 9500 Euclid Ave, Cleveland, OH, USA; wilsons4@ccf.org.

Submitted: July 5, 2018
Accepted: October 21, 2018

Citation: Saikia P, Thangavadivel S, Medeiros CS, Lassance L, de Oliveira RC, Wilson SE. IL-1 and TGF-β modulation of epithelial basement membrane components perlecan and nidogen production by corneal stromal cells. *Invest Ophthalmol Vis Sci*. 2018;59:5589–5598. https://doi.org/10.1167/iovs.18-25202

Purpose. To determine whether (1) the in vitro expression of epithelial basement membrane components nidogen-1, nidogen-2, and perlecan by keratocytes, corneal fibroblasts, and myofibroblasts is modulated by cytokines/growth factors, and (2) perlecan protein is produced by stromal cells after photorefractive keratectomy.

Methods. Marker-verified rabbit keratocytes, corneal fibroblasts, myofibroblasts were stimulated with TGF-β1, IL-1α, IL-1β, TGF-β3, platelet-derived growth factor (PDGF)-AA, or PDGF-AB. Real-time quantitative RT-PCR was used to detect expression of nidogen-1, nidogen-2, and perlecan mRNAs. Western blotting evaluated changes in protein expression. Immunohistochemistry was performed on rabbit corneas for perlecan, alpha-smooth muscle actin, keratocan, vimentin, and CD45 at time points from 1 day to 1 month after photorefractive keratectomy (PRK).

Results. IL-1α or -1β significantly upregulated perlecan mRNA expression in keratocytes. TGF-β1 or -β3 markedly downregulated nidogen-1 or -2 mRNA expression in keratocytes. None of these cytokines had significant effects on nidogen-1, -2, or perlecan mRNA expression in corneal fibroblasts or myofibroblasts. IL-1α significantly upregulated, while TGF-β1 significantly downregulated, perlecan protein expression in keratocytes. Perlecan protein expression was upregulated in anterior stromal cells at 1 and 2 days after −4.5 or −9 diopters (D) PRK, but the subepithelial localization of perlecan became disrupted at 7 days and later time points in −9-D PRK corneas when myofibroblasts populated the anterior stroma.

Conclusions. IL-1 and TGF-β1 have opposing effects on perlecan and nidogen expression by keratocytes in vitro. Proximate participation of keratocytes is likely needed to regenerate normal epithelial basement membrane after corneal injury.

Keywords: cornea, CD45, keratocyte, growth factor, interleukin (IL)-1, transforming growth factor (TGF)-β, wound healing, basement membrane, perlecan, nidogen-1, nidogen-2, vimentin

The corneal epithelial basement membrane (EBM) modulates myofibroblast generation and fibrosis (scarring or "late haze") via regulation of epithelium- and tear film–derived profibrotic growth factors, including TGF-β and platelet-derived growth factor (PDGF).[1–3] Defective corneal EBM regeneration has been shown to underlie the development of myofibroblast-mediated stromal fibrosis that occurs after injuries, such as photorefractive keratectomy[1,2,4] or pseudomonas corneal ulcers,[5] likely by facilitating TGF-β and PDGF penetration into the stroma at sufficient concentrations to drive myofibroblast development from precursor cells. Regeneration of the EBM triggers apoptosis of myofibroblast precursors and mature myofibroblasts by depriving them of a requisite supply of epithelium- and tear film–derived TGF-β and PDGF—allowing repopulation by keratocytes, removal of disordered extracellular matrix produced by the myofibroblasts,[5,6] and restoration of corneal transparency.

Keratocytes, and possibly other stromal cells, contribute to EBM regeneration after corneal injury through the production of EBM components, such as perlecan, nidogens, and laminins.[2,7–10] Similarly, fibroblasts or mesenchymal cells produce basement membrane components in skin, gut, lung, kidney, and other organs that likely contribute to the maintenance or regeneration of basement membranes in those organs.[11–18]

Perlecan is a large, five-domain proteoglycan that is a critical component of basement membranes (BMs), which binds to and crosslinks many extracellular matrix components in BMs and also cell-surface molecules, such as integrens.[19–22] It is a critical organizer of the BMs in many organs and is known to modulate growth factor functions via sequestration by its domain 1.[22] Similarly, nidogens are critical BM components that also interact with other BM components, such as laminins, perlecan, and collagen type IV.[22–24] Although laminins are the major early drivers of BM regeneration via their novel capacity to self-assemble, the addition of perlecan and the nidogens to the regenerating BMs in many organs appears to have a critical role in regeneration of the structurally and functionally mature BM. The cytokine and growth factor regulation of expression of these important BM components has been poorly characterized in the context of wound healing and repair processes. IL-1α,

TGF-β, and PDGF, regulate and orchestrate critical aspects of the wound-healing response of the cornea,[25] including epithelial cell proliferation, motility and differentiation,[26] myofibroblast development,[3,27,28] keratocyte and myofibroblast viability and apoptosis,[29,30] as well as keratocyte and corneal fibroblast production of chemokines,[31] metalloproteinases,[32–34] and collagenases.[35] The purpose of this study was to determine whether IL-1α, TGF-β, or PDGF modulate the production of EBM components nidogen-1, nidogen-2, or perlecan in keratocytes, corneal fibroblasts, or myofibroblasts in vitro. This study also examined perlecan-protein expression and localization in rabbit corneas after –4.5-D photorefractive keratectomy (PRK), when EBM ultrastructure was normally regenerated and the stroma remained transparent, compared with –9-D PRK when the EBM ultrastructure was not regenerated and corneas developed stromal fibrosis.

Methods

Isolation of Rabbit Corneal Keratocytes, Fibroblasts, and Myofibroblasts

Primary keratocytes were isolated and cultured from fresh rabbit corneas (Pel Feeze, Rogers, AR, USA) without serum as previously described with Dulbecco's modified Eagle medium (DMEM; Gibco, Grand Island, NY, USA).[9] Identical methods were used to produce corneal fibroblasts, except the cells isolated from fresh corneas were cultured with 10% fetal bovine serum (FBS; Sigma Aldrich, St. Louis, MO, USA) and fibroblast growth factor (FGF-2, 40 ng/mL; Sigma Aldrich) in DMEM. Corneal myofibroblasts were produced by culturing corneal fibroblasts in DMEM with 1% FBS and 2 ng/mL TGF-β1 (R&D, Minneapolis, MN, USA) for at least 72 hours. The medium was changed every 48 hours in all cultures. In preliminary experiments, advanced DMEM with 2.5 mg/L ascorbic acid (ThermoFisher Scientific, Rockland, IL, USA) was used for the cell culture for quantitative real-time PCR (qRT-PCR).

Western Immunoblotting and Immunohistochemistry (IHC) for Stromal Cell Markers

To verify the specificity of each cultured cell type of the stroma, Western immunoblotting and immunofluorescence were performed to confirm expression of markers specific for these cell types. Primary keratocytes were verified based on their expression of keratocan by Western immunoblotting using a goat keratocan antibody (cat. No.sc33242; Santa Cruz Biotechnology, Santa Cruz, CA, USA) at a 1:2000 dilutions. Mouse anti-goat-HRP conjugated secondary antibody (cat. No. sc2354; Santa Cruz Biotechnology) was used at a dilution 1:5000 in Western blotting. Parallel keratocyte primary cultures were used to verify keratocytes were α-smooth muscle actin (α-SMA). Immunohistochemistry (IHC) was also used for verification of fibroblast and myofibroblast phenotype. The methods for marker IHC of keratocyte-derived corneal fibroblasts or myofibroblasts were to wash the cells with 1× PBS, fix them using IC fixation buffer (1908245; Invitrogen, Carlsbad, CA, USA), block them with 1% BSA in PBS, and incubate cells at room temperature with 1:100 mouse monoclonal antibody anti-vimentin (sc7557; Santa Cruz Biotechnology) or 1:100 goat anti–α-SMA (Dako, Carpentaria, CA, USA) in 1× PBS for 90 minutes, followed by secondary antibody Alexa 488 goat anti-mouse IgG (Invitrogen) or Alexa 488 goat anti-mouse IgG (Invitrogen), respectively, at a dilution of 1:250 for 1 hour. Cells were mounted with Vectashield containing 4′,6-diamidino-2-phenylindole (DAPI; Vector Laboratories, Inc., Burlingame, CA, USA) to allow visualization of nuclei. IHC with secondary antibody alone was used as a negative control in all experiments. Immunostained cultures were photographed with Leica DM5000 microscope equipped with Q-imaging Retiga 4000RV (Surrey, BC, Canada) camera and Image Pro software (Leica Microsystems, Buffalo Grove, IL, USA). Cellular viability of all cell types was also verified using the trypan blue assay.

IHC staining for vimentin+ and α-SMA cells, that were also keratocan– by Western immunoblotting, was performed to verify corneal fibroblast phenotype. IHC for α-SMA+ cells derived from corneal fibroblasts after treatment with 2 ng/mL TGF-β1 for minimum 72 hours was used to confirm myofibroblast phenotype. We also confirmed that myofibroblasts were keratocan– by western immunoblotting. We observed parallel cultures of all cell types for 100% IHC staining and immunoblotting for the corresponding cell-specific markers prior to use of cells for qRT-PCR or Western blotting.

Passage one keratocytes or 2nd to 3rd passage corneal fibroblasts or myofibroblasts were used for all experiments.

Cell Growth Factor Treatment

Cells were treated with or without IL-1α (10 ng/mL), IL-1β (10 ng/mL), TGF-β1 (2 ng/mL), TGF-β3 (10 ng/mL), PDGF-AA (10 ng/mL), or PDGF-AB (10 ng/mL) for 8 or 12 hours, as indicated in the figures. The concentrations of cytokines and growth factors used in these experiments was based on previous studies of effects in the corresponding corneal stromal cells.[9,36–38]

RNA Isolation and Quantitative Real-Time PCR (qRT-PCR)

Total RNA was prepared using the RNeasy Mini Kit (Qiagen, Valencia, CA, USA), reverse transcription and qPCR amplification was performed as described previously.[10] The relative amount of target mRNA was measured using the comparative Ct ($\Delta\Delta^{Ct}$) method by normalizing target mRNA Ct values to those of 18S. The sequences of primers used in this study were described previously.[10] Quantitative real-time experiments were repeated three times and results were consistent in the different experiments. In each case, means for a cytokine or growth factor at each time point were determined from three independent experiments.

Western Blot Analysis

Primary cultures of keratocytes were treated with or without IL-1α (10 ng/mL) or TGF-β1 (2 ng/mL) for 16 hours. Cells were then moved to ice, rinsed three times with 2 mL of ice-cold PBS buffer, and extracted by adding 4 M guanidine chloride containing 1 mM sodium orthovanadate, 10 mM NaF, 10 mM sodium pyrophosphate, 10 mM β-glycerophosphate, 1 mM PMSF (Sigma), 10 μg/mL aprotinin, and protease inhibitor cocktail (Roche, Mannheim, Germany).[19] Extracts were then dialyzed into 50 mM Tris/HCl, pH 7.5, containing 10 mM $CaCl_2$ for 4 hours, and the precipitates (extracellular matrix proteins) were collected and dissolved in 0.1 M Tris-acetate solution (pH 6.0) containing 6 M urea and protease inhibitor. Protein concentrations were determined using the BCA protein assay kit (Thermo Fisher Scientific). For keratocan, a 100 μg protein aliquot was incubated with endo-β-galactosidase (0.1 U/mL; Sigma-Aldrich) in 50 mM sodium phosphate (pH 5.8) at 37°C overnight.[9] After digestion, the protein was lyophilized, dissolved, and underwent Western blot analysis for keratocan. For perlecan Western blots, the dialyzed extract was digested

Investigative Ophthalmology & Visual Science

with 1 mU/mL of heparitinase III (Cat No. H8891; Sigma-Aldrich) at 37°C for 3 hours.[19] For Western blot analysis, 10 µg of cellular protein was separated on 4% to 15% SDS-PAGE gels and then transferred to PVDF membranes for immunoblotting. The membranes were blocked with 5% nonfat milk and probed with primary antibodies at 4°C overnight. The primary antibodies used were anti-perlecan (1:1,000, sc377219; Santa Cruz Biotechnology), anti-nidogen-1 (1:500, AF2570, R&D System), anti-nidogen-2 (1:1000, sc-373859; Santa Cruz Biotechnology), and keratocan (cat. no. sc33242, 1:2000; Santa Cruz Biotechnology). Western blotting for β-actin (1:5,000, A5441; Sigma-Aldrich) was used as a loading control. Western blot analysis was performed using enhanced chemiluminescence for signal detection. Western blot signal intensities were quantified by densitometry using ImageJ software (http://imagej.nih.gov/ij/; provided in the public domain by the National Institutes of Health, Bethesda, MD, USA).

Animals and Surgery

All procedures involving animals were approved by the Institutional Animal Care and Use Committee at the Cleveland Clinic Foundation. All animals were used in accordance with the tenets of the ARVO Statement for the Use of Animals in Ophthalmic and Vision Research. Anesthesia was performed with intramuscular injection of ketamine hydrochloride (30 mg/kg) and xylazine hydrochloride (5 mg/kg). Topical proparacaine hydrochloride 1% (Alcon, Fort Worth, TX, USA) was applied to each eye just prior to surgery. Euthanasia was performed with intravenous injection of 100 mg/kg beuthanasia (Shering-Plough, Kenilworth, NJ, USA) with the animal under general anesthesia.

Female 12- to 15-weeks-old New Zealand white rabbits weighing 2.5 to 3.0 kg were included in this study. One eye of each rabbit was selected at random to have PRK. Contralateral eyes were used for control groups. Rabbits underwent epithelial scrape –4.5-D moderate-injury PRK or –9-D high-injury PRK with a 6-mm diameter ablation zone using a VISX Star S4 IR excimer laser (Abbott Medical Optics, Irvine, CA, USA), according to a previously published method.[10] One drop of Vigamox (Alcon, Ft. Worth, TX, USA) was applied to the PRK and control cornea four times a day until the epithelium healed in eyes that had surgery and control eyes. Time points for –9- or –4.5-D PRK were 1, 2, 4, 7, 14, and 30 days after surgery with three eyes in each group at each time point.

Tissue Fixation, Sectioning, and Immunohistochemistry

The corneoscleral rims were collected, cryopreserved in optimal cutting temperature (OCT) compound (Sakura Fine-Tek, Torrance, CA, USA), within a 24 × 24 × 5-mm mold (Fisher Scientific, Pittsburgh, PA, USA), bisected, and 7-µm thick central corneal cut with a cryostat, as previously described in detail.[5] Sections were placed on 25 × 75 × 1-mm microscope slides (Superfrost Plus; Fisher) and kept at –80°C until IHC was performed. IHC for perlecan was performed using a mouse monoclonal anti-human perlecan antibody (Clone E6; Santa Cruz Biotechnology Inc., Santa Cruz, CA, USA) that was previously shown to work in IHC against rabbit antigen[4] at 1:50 dilution in 1% BSA in PBS for 1 hour at room temperature. The secondary antibody, goat anti-mouse Alexa flour 650, was used at 1:200 dilution in 1% BSA in PBS for 1 hour at room temperature.

Duplex IHC was performed to simultaneously detect the keratocan marker for keratocytes and the α-SMA marker for myofibroblasts. Briefly, for keratocan, a goat anti-human primary antibody raised against keratocan peptide H2N-LRLDGNEIKPPIPIDLVAC-OH (a gift from Winston W. Kao, Cincinnati, OH, USA). For duplex α-SMA with keratocan, a mouse monoclonal anti-human α-SMA clone IA4 (Cat. No-M6851; Dako, Carpinteria, CA, USA) was used. The slides were washed with PBS containing 0.01% Tween-20 and blocked with 5% donkey serum in PBS. The slides were incubated overnight with anti-keratocan antibody at 1:200 dilution and anti–α-SMA antibody at 1:50 dilution in 5% donkey serum containing 0.05% NP-40. The slides were washed three time with PBS containing 0.01% Tween-20 and then incubated at room temperature with secondary antibodies—Alexa Flour 488 donkey anti-goat IgG (Cat# A-11055; ThermoFisher Scientific) and Alexa Fluor 568 donkey anti-mouse IgG (Cat# A10037; ThermoFisher Scientific), both at a dilution of 1:200 in 5% donkey serum containing 0.05%NP-40 for 1 hour. The slides were washed three time with PBS with 0.01% Tween-20 and coverslips were mounted with Vectashield containing DAPI (Vector Laboratories Inc.) to allow visualization of all nuclei. The sections were viewed and photographed with a Leica DM5000 microscope equipped with Q-imaging Retiga 4000RV camera and ImagePro software.

Duplex IHC for vimentin and α-SMA was performed using the method described above, except the primary antibody for vimentin was mouse monoclonal anti-vimentin (Cat. # M7020; Dako) used at 1:50 dilution for 60 minutes and the primary antibody for α-SMA was goat polyclonal anti–α-SMA (Cat. # NB300-978; Novus Biologicals USA, Littleton, CO, USA) used at 1:100 dilution for 60 minutes at room temperature. The secondary antibodies were donkey anti-mouse IgG (H+L) highly cross-adsorbed, Alexa Fluor 488 (Cat. # A21202; Thermo Fisher Scientific) and donkey anti-goat IgG (H+L) cross-adsorbed, Alexa Fluor 568 (Cat. # A11057; Thermo Fisher Scientific), respectively, both used at 1:250 dilution and incubated for 60 minutes at room temperature.

Similarly, duplex IHC for CD45 and α-SMA was performed using the method described above, except slides were blocked with 5% donkey serum in PBS for 90 minutes at room temperature and the primary antibody for CD45 was mouse anti-rabbit CD45 monclonal (Cat. # MCA808GA; Bio-Rad, Hercules, CA, USA) used at 1:50 dilution and the primary antibody for α-SMA was the goat anti–α-SMA polyclonal (Cat. # NB300-978; Novus Biologicals, Centennial, CO, USA) used at 1:100 dilution for 60 minutes at room temperature. The secondary antibodies were the donkey anti-mouse IgG (H+L) highly cross-adsorbed, Alexa Fluor 488 (Cat. # A21202; Invitrogen) used at 1:200 dilution and the donkey anti-goat IgG (H+L) cross-adsorbed, Alexa Fluor 568 (Cat. # A11057; Invitrogen) used at 1:300 dilution, respectively, for 60 minutes at room temperature.

TEM of EBM Ultrastructure

Transmission electron microscopy (TEM) of rabbit corneas at 1 month after –4.5- or –9-D PRK was performed by previously published methods[39,40] using a Philips CM12 transmission electron microscope operated at 60 kV (FEI Company, Hillsboro, OR, USA).

Statistical Analysis

A sample size of three was used in all experiments. All data are represented as the mean ± SD, and statistical significance was determined using Dunnett's test from three or more independent experiments and the growth factor–treated groups were compared with the control groups. A $P < 0.05$ was considered to be a statistically significant difference.

Investigative Ophthalmology & Visual Science

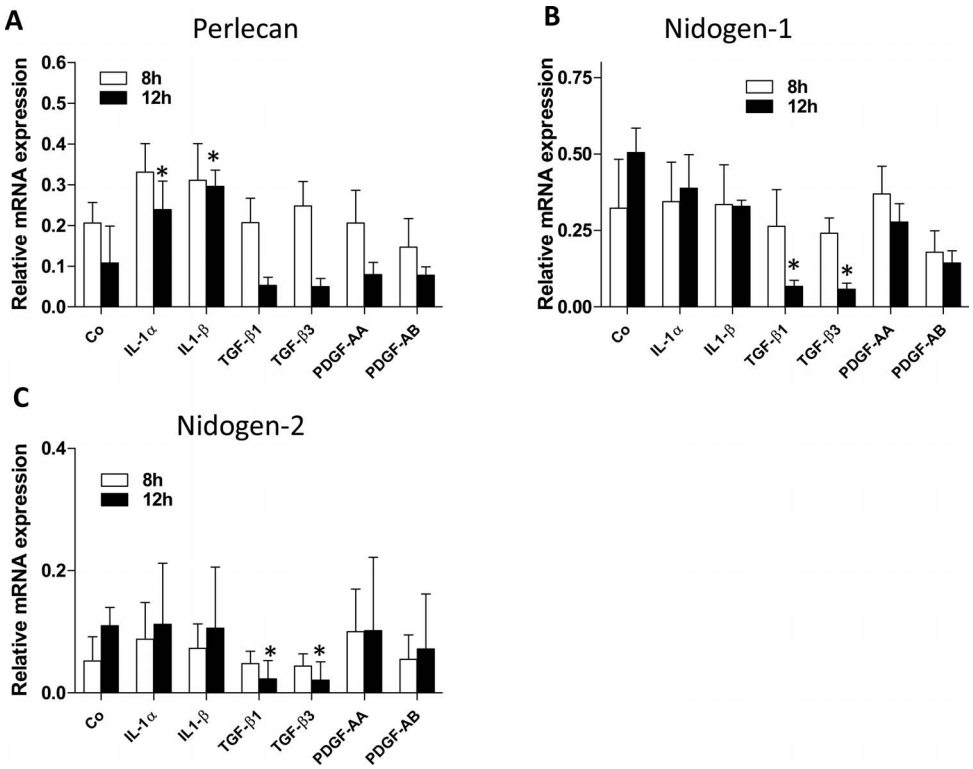

Figure 1. EBM component mRNA expression in primary cultures of rabbit keratocytes in presence of different cytokines/growth factors. Keratocan+ keratocytes were cultured and treated with 10 ng/mL IL-1α, 10 ng/mL IL-1β, 2 ng/mL TGF-β1, 10 ng/mL TGF-β3, 10 ng/mL PDGF-AA, or 10 ng/mL PDGF-AB for 8 or 12 hours. Expression of perlecan (**A**), nidogen-1 (**B**), and nidogen-2 (**C**) mRNA was measured by qRT-PCR and normalized to 18S rRNA as described in the material and methods section. "Co" represents primary cultured keratocan + keratocytes in the medium without added cytokines or growth factors. Data for each BM component and each cytokine or growth factor are presented as means of three independent experiments and statistical comparisons were made between vehicle-treated control keratocytes and cytokine- or growth factor–treated keratocytes at the same time points. No comparisons were made between the 8- and 12-hour time points.

Results

Analysis of Growth Factors/Cytokines Effects on Nidogen-1, Nidogen-2, or Perlecan mRNA with Real-Time PCR

Initially, a series of cytokines and growth factors known to be critical modulators of the early corneal wound healing response (IL-1α, IL-1β, TGF-β1, TGF-β3, PDGF-AA, or PDGF-AB) were screened for modulation of the mRNAs of key BM components by marker-verified keratocytes, keratocyte-derived corneal fibroblasts, or keratocyte-derived myofibroblasts in vitro. Two different time points, 8 and 12 hours of cytokine exposure were included and the data for each cytokine or growth factor were obtained by calculating the means from three independent experiments (Fig. 1). At each time point of exposure, 8 or 12 hours, the cytokine- or growth factor–treated keratocytes were compared statistically to vehicle-treated keratocytes ("Co" in Fig. 1).

In keratocytes, perlecan mRNA was significantly increased in response to 10 ng/mL IL-1α or 10 ng/mL IL-1β at 12 hours compared with the control cultures without IL-1α or -1β (Fig. 1A). There was a trend for each cytokine to increase perlecan mRNA at 8 hours in keratocytes that did not reach statistical significance compared with control cultures (Fig. 1A). There were trends for 2 ng/mL TGF-β1 or 10 ng/mL TGF-β3 exposure for 12 hours to decrease perlecan mRNA expression in keratocytes (Fig. 1A) but these changes did not reach statistical significance compared with control keratocyte cultures. Neither 10 ng/mL PDGF-AA or 10 ng/mL PDGF-BB had an effect on perlecan mRNA expression with 8 or 12 hours of exposure (Fig. 1A). In contrast, 2 ng/mL TGF-β1 or 10 ng/mL TGF-β3 significantly inhibited expression of nidogen-1 (Fig. 1B) or nidogen-2 (Fig. IC) mRNA in the keratocytes after 12 hours of exposure compared with control cultures. IL-1α, IL-1β, PDGF-AA, or PDGF-AB did not have significant effects on nidogen-1 (Fig. 1B) or nidogen-2 (Fig. IC) mRNA expression compared with controls with either 8 or 12 hours of exposure.

None of the tested cytokines had significant effects on perlecan mRNA expression in corneal fibroblasts or myofibroblasts (not shown). Similarly, none of the tested cytokines had significant effects on nidogen-1 or -2 mRNA expression in corneal fibroblasts or myofibroblasts (not shown). Also, use of DMEM culture medium with 2.5 mg/L ascorbic acid in preliminary experiments showed no difference from standard DMEM on qRT-PCR results and, therefore, only the nonascorbic acid results were reported.

These qRT-PCR experiments were repeated three times with each stromal cell types and the results were consistent in the different experiments.

Analysis of Perlecan, Nidogen-1, Nidogen-2 Proteins With Western Immunoblotting in Keratocytes

Western immunoblotting was used to confirm that cells exposed to IL-1a or TGFβ-1 were keratocan+ keratocytes at the beginning of the exposure (Fig. 2A). Western immunoblot-

Investigative Ophthalmology & Visual Science

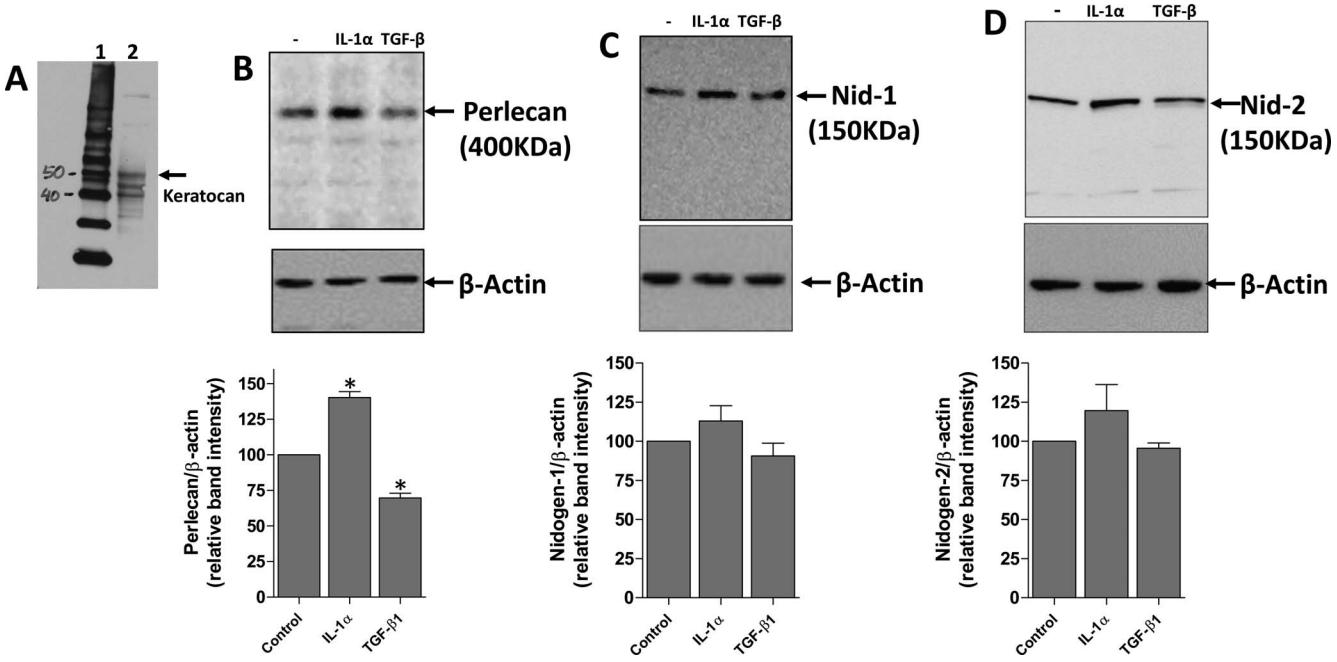

Figure 2. Regulation of EBM component protein expression by IL-1α and TGF-β1 in primary rabbit keratocytes. Primary keratocan+ keratocytes were cultured and treated with 10 ng/mL IL-1α, 2 ng/mL TGF-β1, or left untreated for 16 hours. Keratocytes to be used in the experiments were lysed and keratocan of the expected size (50 kDa[45]) was detected (**A**) to confirm these cells were keratocan+ keratocytes at the beginning of the exposure. (**B**) Perlecan, (**C**) nidogen-1, and (**D**) nidogen-2 expression detected by Western blot. Cell extracts used for perlecan Western blots were treated with heparitinase III, as was described in the methods. β-actin was used as a loading control for each experiment. A representative Western blot of the three performed for each BM component is shown. The graphs beneath each Western blot was obtained by densitometry analysis of the bands from each of the three Western blots from different experiments. *The change in BM protein was statistically significant ($P < 0.05$) compared with the control keratocytes.

ting was then used to confirm the effects of 10 ng/mL IL-1α or 2 ng/mL TGF-β1 in modulating BM protein expression by keratocan+ (Fig. 2A) keratocytes after 16 hours in vitro. An example Western blot experiment for each BM component is shown in Figures 2B to 2D. The graph below each BM Western blot in Figures 2B to 2D was obtained by analyzing band signal intensities with densitometry using ImageJ software in three independent Western blot experiments using three independent sets of cultures generated from rabbit corneas and then determining the mean ± SD of band intensity relative to the controls.

All three BM proteins of the expected size (perlecan,[19] Fig. 2B; nidogen-1,[23] Fig. 2C; and nidogen-2,[24] Fig. 2D) were expressed in keratocytes. IL-1α increased the expression of perlecan protein in keratocytes (Fig. 2B). There was a trend for IL-1α to increase nidogen-1 (Fig. 2C) or -2 (Fig. 2D) protein expression in keratocytes after 16 hours of exposure, but the difference compared with control keratocytes did not reach statistical significance.

TGF-β1, in contrast, inhibited the expression of perlecan protein in keratocytes after 16 hours of exposure (Fig. 2B). There was a trend for TGF-β1 to decrease nidogen-1 (Fig. 2C) or -2 (Fig. 2D) protein expression in keratocytes after 16 hours of exposure, but the decreases did not reach statistical significance compared with the control keratocytes.

Analysis of Perlecan Protein Expression in the Injured Corneas Using IHC

To complement the in vitro experiments, –4.5- or –9-D PRK was performed in rabbit corneas to study perlecan expression in situ by the stromal cells with IHC during the subsequent corneal wound healing response. In rabbit corneas that had –4.5- or –9-D PRK, the epithelium closed around 4 days after surgery. In corneas that have –4.5-D PRK, the EBM has been shown to fully regenerate to normal morphology with lamina lucida and lamina densa at 8 to 10 days after surgery.[6]

IHC was performed to detect perlecan in unwounded corneas at 1, 2, 4, 7, 14, and 30 days after –9- or –4.5-D PRK (Fig. 3). By 1 day, and especially at 2 days, after either –9- or –4.5-D PRK, perlecan protein was upregulated in anterior stromal cells (Figs. 3C–F) compared with the control unwounded corneas. As the epithelium was healing, a subepithelial concentration of perlecan appeared at the nascent EBM in either –9- or –4.5-D corneas (Figs. 3E, 3F). At 4 days after PRK, perlecan production in the anterior stromal cells was detectible, but less than at 2 days after PRK in either the –9- or –4.5-D PRK groups (Figs. 3G, 3H). A layer of subepithelial perlecan at the site of the nascent EBM persisted in both groups at 4 days. By 7 days after PRK, a difference was noted in the subepthelial layer of perlecan where the nascent EBM was regenerating in the –9-D PRK corneas destined to develop subepithelial fibrosis (Fig. 3I). This layer became less prominent and had skipped areas with no detectible perlecan in all corneas analyzed in the 7 day –9-D PRK group compared with the –4.5-D PRK group (Fig. 3J). This difference in the nascent EBM perlecan became even more prominent by 14 days after PRK, with no EBM perlecan detectible in the –9-D PRK group (Fig. 3K) in any of the corneas analyzed and persistent EBM perlecan in all of the –4.5-D PRK corneas analyzed (Fig. 3L). Prominent cells with perlecan were present in the anterior stroma at 14 days after –9-D PRK (Fig. 3K), but not in –4.5-D PRK corneas at 14 days after surgery (Fig. 3L). It is known from prior work[1,4,5] that α-SMA– myofibroblast precursor cells develop to become α-SMA+ myofibroblasts in the subepi-

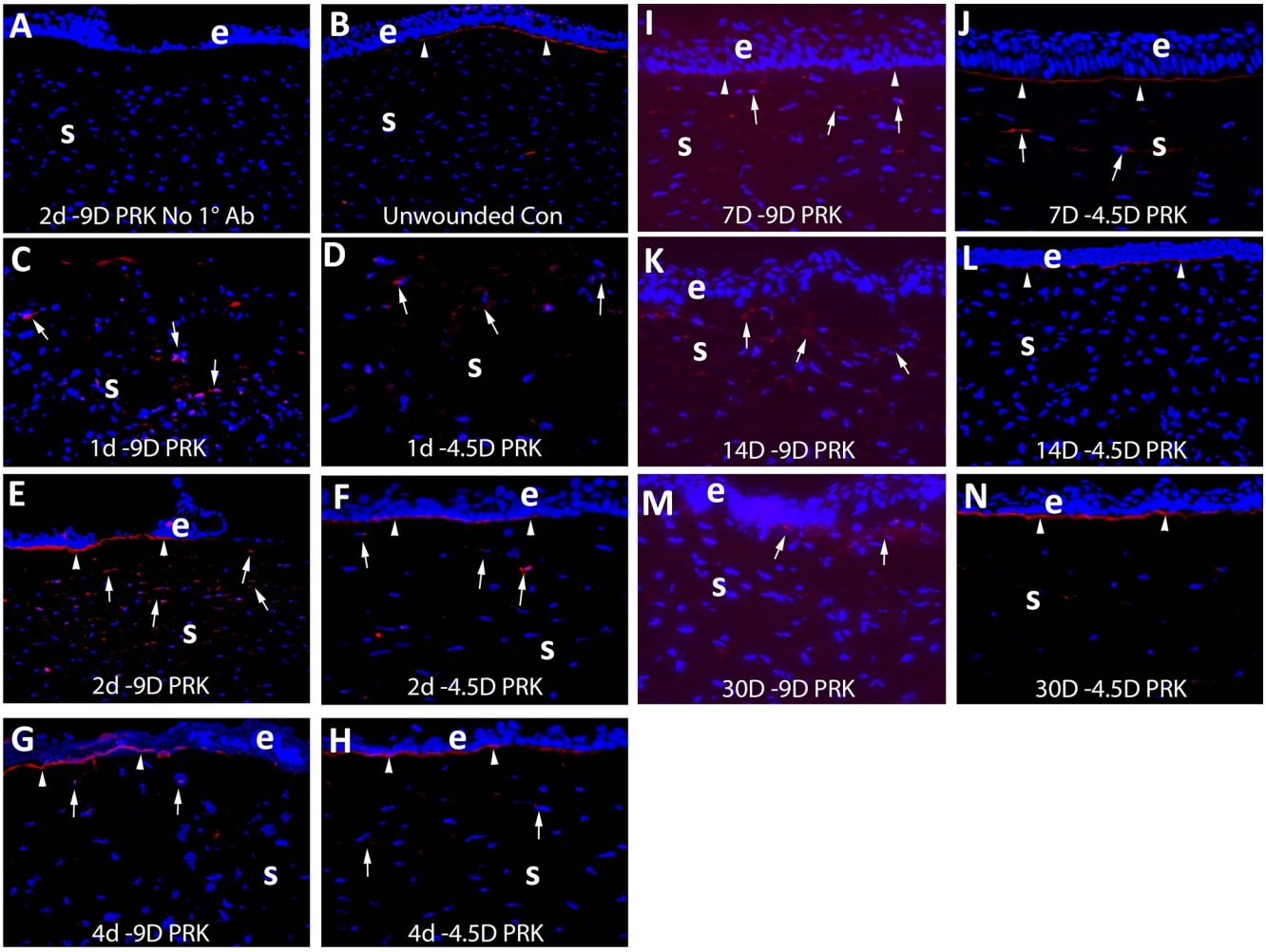

Figure 3. Immunohistochemistry for perlecan protein expression in control unwounded corneas and at time points after –4.5- and –9-D PRK in rabbits. e is epithelium and S is stroma in each panel. Blue is DAPI staining of all nuclei in all panels. In each case, the panel shown is representative of the results noted in three corneas at each time point in each group. (**A**) Example control staining (this example at 2 days after –9-D PRK) with no primary antibody. (**B**) In unwounded control corneas perlecan was detected in the EBM (*arrowheads*) but little was detected in stromal cells. At (**C**) 1 day after –9-D PRK (**D**) 1 day after –4.5-D PRK, perlecan protein production was present in some stromal cells (*arrows*). At (**E**) 2 days after –9-D PRK, (**F**) 2 days after –4.5-D PRK, (**G**) 4 days after –9-D PRK, or (**H**) 4 days after –4.5-D PRK there was similar perlecan in the nascent EBM (*arrowheads*) and stromal cells (*arrows*). At 7 days after –9-D PRK, a change was noted in subepithelial EBM perlecan (*arrowheads*) in the (**I**) –9-D PRK corneas compared with the (**J**) –4.5-D PRK corneas. At 14 days, after the difference in the subepithelial perlecan (*arrowheads*) between (**K**) –9-D and (**L**) –4.5-D PRK was even more pronounced. Perlecan was detected in anterior stromal cells in both groups (*arrows*). At (**M**) 30 days after –9-D PRK there continued to be no subepithelial linear EBM perlecan, although perlecan was detected in cells in the anterior stroma (*arrows*). In contrast, in corneas (**N**) at 30 days after –4.5-D PRK, the linear EBM-associated perlecan (*arrowheads*) was present and there was relatively little perlecan present in stromal cells. Magnification ×200 in all panels.

thelial stroma at 14 days after –9-D PRK (not shown) and some of those perlecan+ cells in the anterior stroma in Figure 3K are likely those developing cells. Similarly, at 30 days after –9-D PRK (Fig. 3M), there was no defined subepithelial layer of perlecan and prominent cells expressing perlecan were present in the anterior stroma. This contrasts to –4.5-D PRK corneas at 30 days after surgery (Fig. 3N) where a prominent layer of perlecan was present beneath the epithelium and few cells in the anterior stroma expressed perlecan. At this time point after –9-D PRK, all rabbit corneas uniformly had subepithelial fibrosis (scarring or haze, not shown) and a dense subepithelial layer of α-SMA+ myofibroblasts (see Figs. 4, 5) and the detected stromal perlecan was likely in these cells and may also have been present in other α-SMA– stromal cells.

Multiplex IHC to Detect Keratocan, α-SMA, Vimentin, and CD45 in Corneas at 1 Month After PRK

To study the localization of α-SMA+ myofibroblasts and keratocan+ keratocytes in the stroma at 1 month after –4.5-D PRK, compared with –9-D PRK, duplex IHC was performed (Fig. 4). In the –4.5-D PRK corneas the stroma was filled with keratocan and keratocan+ keratocytes without α-SMA+ cells (Fig. 4A). Conversely, in –9-D PRK corneas, there was a layer of α-SMA+ myofibroblasts immediately posterior to the epithelium in all three corneas analyzed (Fig. 4B). Further posterior in the stroma, keratocan+ keratocytes were prominent in the –9-D PRK corneas but keratocan stromal staining appeared less homogeneous than in the –4.5-D PRK corneas. Interestingly, between the α-SMA+ myofibroblasts and the keratocan+

Investigative Ophthalmology & Visual Science

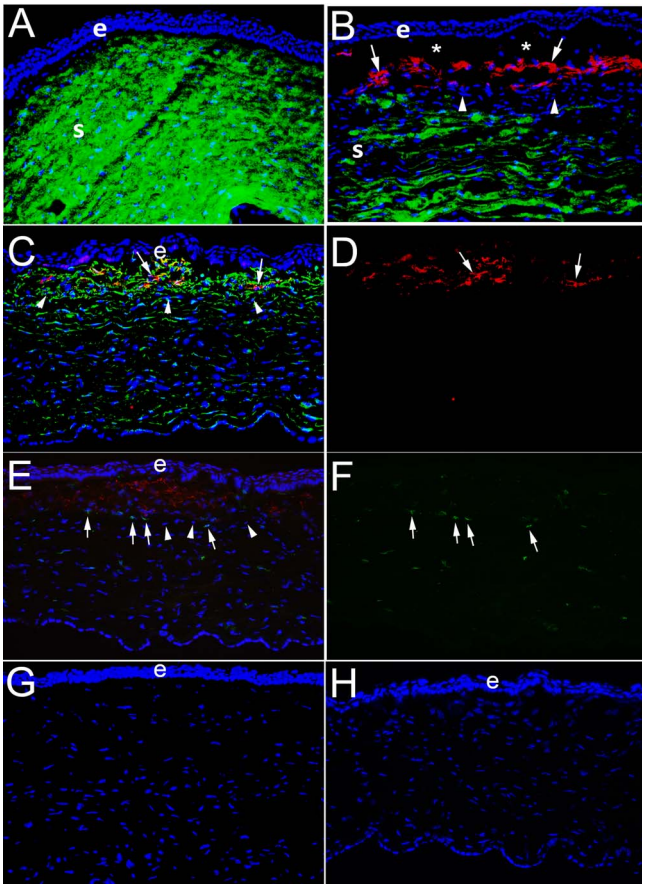

Figure 4. IHC for the keratocyte marker keratocan, myofibroblast marker α-SMA, vimentin, and CD45 in corneas at 1 month after PRK in rabbits. e is epithelium and S is stroma. (**A**) At 1 month after –4.5-D PRK, duplex IHC shows keratocan[41] (*green*) is homogeneously distributed in keratocytes and throughout the stroma and no α-SMA is detected. (**B**) In contrast, at 1 month after –9-D PRK, when corneas have dense subepithelial fibrosis at the slit lamp (not shown) duplex straining shows α-SMA (*red*)+ keratocan– myofibroblasts (*arrows*) present in the subepithelial anterior stroma. Beneath this layer of myofibroblasts, there are keratocan+ α-SMA– keratocytes, although the keratocan staining in the stroma is less homogeneous than in –4.5-D PRK corneas. *Artifactual separation of the epithelium from the stroma that commonly occurs during cryostat sectioning of corneas with anterior myofibroblasts and fibrosis due to poor adhesion between the epithelium and the stromal surface. In a control IHC for keratocan and α-SMA on a section from a –9-D PRK cornea at 1 month after surgery in which both primary antibodies were excluded there was no nonspecific staining (not shown). (**C**) Duplex IHC for vimentin and SMA in a –9-D PRK cornea at 1 month after surgery shows α-SMA+ myofibroblasts (*arrows*) are also vimentin+, as expected. Keratocytes deeper in the cornea are weakly vimentin+. Also, most, if not all, of the cells in the band (*arrowheads*) between myofibroblasts and keratocytes seen in (**B**) are also vimentin+. (**D**) The same image as (**C**), except showing only α-SMA+ red, better shows the position of the myofibroblasts (*arrows*). (**E**) Duplex IHC for α-SMA and CD45 in a –9-D PRK cornea at one month after surgery shows some of the cells within the band beneath the α-SMA+ myofibroblasts are CD45+ (*arrows*), but others are CD45– (*arrowheads*). Some α-SMA+ myofibroblasts are also CD45+, indicating these myofibroblasts likely developed from fibrocytes that migrated into the cornea. Keratocytes are CD45–, but some CD45+ cells are noted in this posterior area that are bone marrow–derived cells that migrated into the stroma after injury. (**F**) The same image as (**E**), except showing only CD45+ cells and it better shows they are present beneath the anterior zone populated with α-SMA+ myofibroblasts, but also among the α-SMA+ myofibroblasts in the anterior stroma and keratocytes in the posterior stroma. (**G**) Control duplex IHC for vimentin and α-SMA without either primary antibody shows no nonspecific staining. (**H**) Control duplex IHC for CD45 and α-SMA without either primary antibody shows no nonspecific staining. All magnifications are ×200.

keratocytes was a thin band of α-SMA– keratocan– cells. Duplex IHC for vimentin and α-SMA in a –9-D PRK cornea at 1 month (Figs. 4C, 4D) showed α-SMA+ myofibroblasts (arrows) were also vimentin+, as expected. Keratocytes deeper in the cornea were also weakly vimentin+. Most, if not all, of the cells in the band between myofibroblasts (arrows in Figs. 4C, 4D) and keratocytes (arrowheads) were also vimentin+. Duplex staining for α-SMA and CD45 (Figs. 4E, 4F) showed some, but not all, of the cells in the band beneath the myofibroblasts were CD45+. Because corneal fibroblasts and keratocytes are CD45–, these cells likely included fibrocytes and their progeny that were undergoing differentiation into myofibroblasts. Some myofibroblasts were also CD45+, and these were myofibroblasts that differentiated from fibrocytes and retained the CD45 marker at this point 1 month after surgery, as was shown in the mouse model of fibrosis.[41] Figures 4G and 4F show control IHC without primary antibodies for vimentin/α-SMA and CD45/α-SMA, respectively, showing there was no nonspecific staining. Similar no primary antibody controls for α-SMA/keratocan did not show nonspecific staining (not shown).

Transmission Electron Microscopy to Confirm EBM Ultrastructure at 1 Month After PRK

An unwounded control cornea has normal lamina lucida and lamina densa beneath the epithelium (Fig. 5A). At 1 month after –4.5-D PRK (Fig. 5B), lamina lucida and lamina densa (arrowheads) of the EBM were regenerated and appeared similar to the normal unwounded cornea. Note the uniformity of the diameter of the collagen fibrils in the stroma that has a critical role in corneal transparency. At 1 month after –9-D PRK (Fig. 5C), there was no EBM lamina lucida or lamina densa detected and the anterior stroma was occupied by layers of myofibroblasts filled with prominent endoplasmic reticulum and there was disorganized extracellular matrix between the cells. These cells were the same ones that were α-SMA+ in Figure 4C and were perlecan+ in Figure 3M.

Discussion

The results of this study conclusively demonstrate that IL-1α upregulates perlecan mRNA (Fig. 1A) and protein (Fig. 2B) and IL-1β upregulates perlecan mRNA (Fig. 1A) in keratocytes. Conversely, TGF-β1 and -β3 significantly downregulated nidogen-1 and -2 mRNA (Figs. 1B and 1C) in keratocytes and there was a trend for TGF-β1 and -β3 to downregulate perlecan mRNA (Fig. 1A) in keratocytes, although the latter did not reach statistical significance in this study. However, TGF-β1 did downregulate perlecan protein in keratocytes (Fig. 2B) and there was a trend for TGF-β1 to downregulate nidogen-1 and -2 protein in keratocytes (Figs. 2C, 2D). Thus, this study has again shown IL-1 and TGF-β1 having opposing effects on an important aspect of the corneal wound healing response—in this case epithelial BM component production—as was previously shown for myofibroblast viability.[30] This study is an important demonstration of cytokine and growth factor regulation of perlecan and nidogens production during wound healing. Importantly, none of the cytokines or growth factors that were studied significantly regulated perlecan, nidogen-1, or -2 mRNA production in vitro in corneal fibroblasts or myofibroblasts. A prior study found perlecan mRNA expression was increased by IL-1α in hippocampal glial cultures.[20] Ichimaru and coworkers,[42] demonstrated that TGF-β1 induced

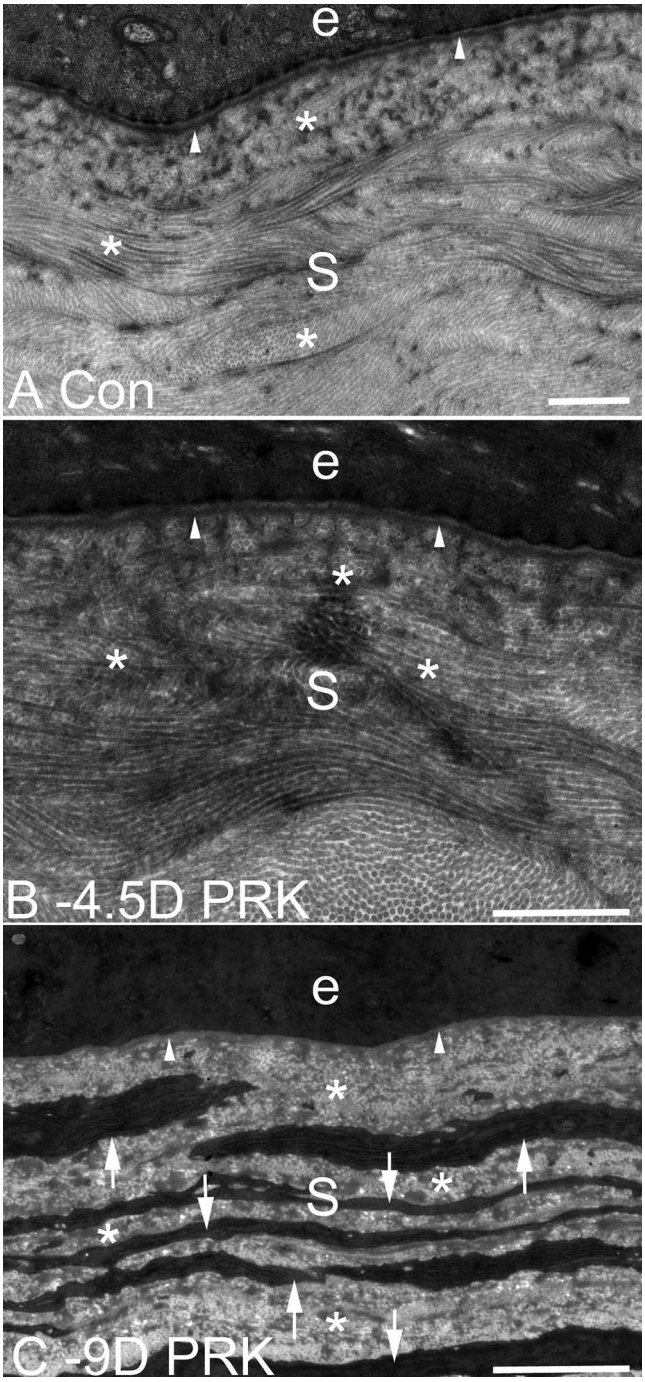

Figure 5. TEM of EBM ultrastructure and the anterior stroma at 1 month after –9- or –4.5-D PRK, or in control unwounded, rabbit corneas. (**A**) In an unwounded cornea, lamina lucida, and lamina densa (*arrowheads*) are present beneath the epithelium (e). S is stroma in all panels. (**B**) At 1 month after –4.5-D PRK, the normal lamina lucida and lamina densa (*arrowheads*) of the EBM are regenerated beneath the epithelium (e). There are no cells seen in the subepithelial stroma with high levels of rough endoplasmic reticulum suggestive of myofibroblasts. *In panels (**A**) and (**B**), note the uniform diameter of collagen fibrils throughout the stroma, with some seen longitudinally and others cut transversely. (**C**) At 1 month after –9-D PRK, normal lamina lucida and lamina densa cannot be detected (*arrowheads*) beneath the epithelium (e) and the subepithelial stromal is filled with layered myofibroblasts (*arrows*, and same cells seen in IHC for α-SMA shown in [**C**]) with large amounts of rough endoplasmic reticulum. Note the relative disorganization of the collagen fibrils in the extracellular matrix (*) between the myofibroblast cells compared with the fibrils with uniform thickness and regular distribution in the stroma of panels (**A**) and (**B**). *Magnification bars* are 1 μm in each panel.

perlecan deposition by chronic obstructive pulmonary disease airway smooth muscle cells. Warren and coworkers,[43] found that TNF-α, but not TGF-β, upregulated production of perlecan in prostrate stromal cell lines. Thus, there appears to be variability in the response to TGF-β in stromal cells from different organs.

This study also found that perlecan protein was upregulated (Figs. 3E, 3F) in anterior stromal cells in situ during the first few days after –9-D PRK (that triggers anterior stromal fibrosis) and –4.5-D PRK (that does not trigger anterior stromal fibrosis) and a thin layer of perlecan appeared beneath the healed epithelium at the site of the nascent regenerating EBM. It is hypothesized that IL-1α and -1β released from the injured and healing epithelium into the stroma triggers this upregulation in stromal cells. Importantly, little perlecan protein was detected in the epithelium in situ after injury—supporting the hypothesis that stromal cells are the major contributor of this critical EBM component during EBM regeneration after corneal injury.[2,10] It is known from prior studies that development of an ultrastructurally mature epithelial BM with lamina lucida and lamina densa does not appear until 8 to 10 days after –4.5-D PRK.[6] Up to 4 days after PRK, perlecan localization during EBM regeneration appeared similar in the –9- and –4.5-D PRK groups. However, beginning at 7 days after surgery (Fig. 3I) the linear layer of subepithelial perlecan appeared to break down in –9-D PRK corneas. By 14 and 30 days after –9-D PRK (Figs. 3K, 3M) this subepithelial perlecan layer was undetectable, in contrast to the well-delineated layer in the –4.5-D PRK corneas (Figs. 3L, 3N). This occurred despite the presence of perlecan+ anterior stromal cells in the –9-D PRK corneas at these time points. These perlecan+ stromal cells likely include myofibroblast precursor cells that are predominately α-SMA– at 14 days after –9-D PRK but which continue development into mature α-SMA+ myofibroblasts by 30 days after –9-D PRK (Fig. 4B).[6,42,43] These in situ results are consistent with prior in vitro results in cultured cells that showed that myofibroblasts produce perlecan protein.[9] However, even though these myofibroblasts were in proximity to the nascent EBM (Figs. 3K, 3M), the EBM perlecan that appeared to be within the nascent regenerating EBM up to 4 days after –9-D PRK (Fig. 3G) became disorganized and undetectable immediately beneath the epithelium at 14 and 30 days after –9-D PRK (Figs. 3K, 3M), in contrast to corneas that had –4.5-D PRK at these same time points after surgery (Figs. 3L, 3N). Corneal fibroblasts do not produce perlecan in vitro.[9] These results further support the hypothesis that direct participation of keratocytes is necessary for normal regeneration of the EBM.[1,2,4,8–10]

Importantly, the results in Figures 1 and 2 relate to individual effects of growth factors and cytokines on cultured keratocytes. Figure 3, on the other hand, relates to the more complex in situ situation where the response is regulated by not only the individual cytokines and growth factors tested in Figures 1 and 2, but also likely other cytokine and growth factors and cellular-matrix interactions at play in the organ after injury.

Experiments, such as those in Figure 4, had not been possible until now because there was no antibody available for IHC for keratocan in rabbit corneas in situ after injury.[44] Figure 4A shows the uniform distribution of keratocan in the keratocytes and surrounding stroma of the unwounded rabbit cornea. At 1 month after high correction –9-D PRK that caused

severe scarring (fibrosis), the anterior cornea beneath the epithelium was populated by α-SMA+ myofibroblasts (Fig. 4B), which could also be noted in multiple layers beneath the epithelium when the cornea was imaged with TEM (Fig. 5C). The distribution of keratocan in the posterior stroma of the fibrotic cornea at 1 month was also less homogeneous (Fig. 4B). Interestingly, between the α-SMA+ myofibroblasts and the keratocan+ keratocytes, there was a band of α-SMA− keratocan− cells. Figure 4C demonstrates that many of the cells in that band were vimentin+. Figure 4E shows that in this cornea 25% of the cells in the α-SMA− keratocan− band were also CD45+. Cells in this band that were vimentin+ CD45+ were likely fibrocytes or their progeny that were being driven by TGF-β from the overlying epithelium (in the absence of a mature EBM; Fig. 5C) to develop into myofibroblasts.[41] Only one or two CD45+ cells were detected in sections from unwounded normal corneas (not shown).[41] The cells that were vimentin+ CD45− in this intermediate band were likely corneal fibroblasts that developed from keratocytes, also under the influence of TGF-β. Other CD45+ bone marrow–derived cells that could have been in this band of α-SMA− keratocan− cells included monocytes and macrophages. Interestingly, in recent studies of posterior corneal injury to Descemet's membrane it was noted that a similar keratocan− α-SMA− band of cells was present anterior to the posterior fibrosis and posterior to keratocan+ keratocytes that were also shown to be primarily corneal fibroblasts, fibrocytes, and fibrocyte progeny (Mederois and Wilson, unpublished data, 2018). Studies are in progress to further characterize this transitional zone that appears to contribute myofibroblasts to fibrotic areas of injured corneas from both keratocyte- and fibrocyte-derived precursor cells.

Studies have suggested that defective EBM regeneration in the higher injury –9-D PRK (in contrast to lower injury –4.5-D PRK) allows for continued epithelium-derived TGF-β1 penetration into the stroma that drives myofibroblast development from precursors.[1–6,43,45] It appears from the current study that this same epithelium-derived TGF-β1 could participate in inhibiting mature BM regeneration by downregulating perlecan and nidogen production by keratocytes. Thus, the TGB-β1 acts at least at two levels to promote fibrosis in this high-injury PRK model, by (1) inhibiting regeneration of mature EBM, the lack of which would tend to facilitate ongoing penetration of epithelium-derived TGF-β1 into the stroma, and (2) promoting the development of mature myofibroblasts from both keratocyte-derived and bone marrow–derived precursor cells.[45] Conversely, IL-1α or -1β trigger myofibroblast apoptosis when these cells are in a low TGF-β milieu.[30] By stimulating perlecan and nidogen production by keratocytes, IL-1 presumably tends to promote EBM regeneration that inhibits stromal myofibroblast development and promotes apoptosis of any mature myofibroblasts that develop. The multiple and complex interactions between TGF-β and IL-1, as well as those of other growth factors and cytokines, that orchestrate the response to corneal injury seem to be at the heart of the regenerative versus fibrotic corneal repair pathways, and further investigation is needed to understand these important interplays.

The present work demonstrates that IL-1 and TGF-β, critical regulators of the overall wound healing response in the cornea, have important roles in modulating the production of perlecan and nidogens in the cornea during the wound healing response to injury that determines whether the EBM regenerates normally, and, therefore, whether the cornea heals with transparency or fibrosis. It seems likely these master regulators play similar roles in other organs where regenerative versus fibrotic repair is important in the pathophysiology of disease.

Acknowledgments

The authors thank Winston Kao, PhD, for the keratocan antibody used in this study.

Supported in part by US Public Health Service grants RO1EY10056 (SEW) and P30-EY025585 from the National Eye Institute, National Institutes of Health, Bethesda, MD and Research to Prevent Blindness, New York, NY. Research reported in this publication was supported by the Office of the Director, National Institutes of Health under award number S10RR031536 for transmission electron microscopy. Luciana Lassance supported by NEI training grant T32 EY007157.

Disclosure: **P. Saikia**, None; **S. Thangavadivel**, None; **C.S. Medeiros**, None; **L. Lassance**, None; **R.C. de Oliveria**, None; **S.E. Wilson**, None

References

1. Torricelli AA, Santhanam A, Wu J, Singh V, Wilson SE. The corneal fibrosis response to epithelial-stromal injury. *Exp Eye Res*. 2016;142:110–118.
2. Wilson SE, Marino GK, Torricelli AAM, Medeiros CS. Injury and defective regeneration of the epithelial basement membrane in corneal fibrosis: a paradigm for fibrosis in other organs? *Matrix Biol*. 2017;64:17–26.
3. Singh V, Jaini R, Torricelli AA, et al. TGF beta and PDGF-B signaling blockade inhibits myofibroblast development from both bone marrow-derived and keratocyte-derived precursor cells in vivo. *Exp Eye Res*. 2014;121:35–40.
4. Torricelli AA, Singh V, Santhiago MR, Wilson SE. The corneal epithelial basement membrane: structure, function, and disease. *Invest Ophthalmol Vis Sci*. 2013;54:6390–6400.
5. Marino GK, Santhiago MR, Santhanam A, et al. Epithelial basement membrane injury and regeneration modulates corneal fibrosis after pseudomonas corneal ulcers in rabbits. *Exp Eye Res*. 2017;161:101–105.
6. Marino GK, Santhiago MR, Santhanam A, Torricelli AAM, Wilson SE. Regeneration of defective epithelial basement membrane and restoration of corneal transparency after photorefractive keratectomy. *J Refract Surg*. 2017;33:337–346.
7. Hassell JR, Schrecengost PK, Rada JA, SundarRaj N, Sossi G, Thoft RA. Biosynthesis of stromal matrix proteoglycans and basement membrane components by human corneal fibroblasts. *Invest Ophthalmol Vis Sci*. 1992;33:547–557.
8. Torricelli AA, Marino GK, Santhanam A, Wu J, Singh A, Wilson SE. Epithelial basement membrane proteins perlecan and nidogen-2 are up-regulated in stromal cells after epithelial injury in human corneas. *Exp Eye Res*. 2015;134:33–38.
9. Santhanam A, Torricelli AA, Wu J, Marino GK, Wilson SE. Differential expression of epithelial basement membrane components nidogens and perlecan in corneal stromal cells in vitro. *Mol Vis*. 2015;21:1318–1327.
10. Santhanam A, Marino GK, Torricelli AA, Wilson SE. EBM regeneration and changes in EBM component mRNA expression in stromal cells after corneal injury. *Mol Vis*. 2017;23:39–51.
11. Marinkovich MP, Keene DR, Rimberg CS, Burgeson RE. Cellular origin of the dermal-epidermal basement membrane. *Dev Dyn*. 1993;197:255–267.
12. Fox JW, Mayer U, Nischt R, et al. Recombinant nidogen consists of three globular domains and mediates binding of laminin to collagen type IV. *EMBO J*. 1991;10:3137–3146.
13. El Ghalbzouri A, Jonkman MF, Dijkman R, Ponec M. Basement membrane reconstruction in human skin equivalents is regulated by fibroblasts and/or exogenously activated keratinocytes. *J Invest Dermatol*. 2005;124:79–86.

14. Simon-Assmann P, Bouziges F, Arnold C, Haffen K, Kedinger M. Epithelial-mesenchymal interactions in the production of basement membrane components in the gut. *Development*. 1988;102:339–347.
15. Fleischmajer R, Utani A, MacDonald ED, et al. Initiation of skin basement membrane formation at the epidermo-dermal interface involves assembly of laminins through binding to cell membrane receptors. *J Cell Sci*. 1998;111(Pt 14):1929–1940.
16. El Ghalbzouri A, Ponec M. Diffusible factors released by fibroblasts support epidermal morphogenesis and deposition of basement membrane components. *Wound Repair Regen*. 2004;12:359–367.
17. Smola H, Stark HJ, Thiekotter G, Mirancea N, Krieg T, Fusenig NE. Dynamics of basement membrane formation by keratinocyte-fibroblast interactions in organotypic skin culture. *Exp Cell Res*. 1998;239:399–410.
18. Furuyama A, Kimata K, Mochitate K. Assembly of basement membrane in vitro by cooperation between alveolar epithelial cells and pulmonary fibroblasts. *Cell Struct Funct*. 1997;22:603–614.
19. Melrose J, Roughley P, Knox S, Smith S, Lord M, Whitelock J. The structure, location, and function of perlecan, a prominent pericellular proteoglycan of fetal, postnatal, and mature hyaline cartilages. *J Biol Chem*. 2006;281:36905–36914.
20. Garcia de Yebenes E, Ho A, Damani T, Fillit H, Blum M. Regulation of the heparan sulfate proteoglycan, perlecan, by injury and interleukin-1alpha. *J Neurochem*. 1999;73:812–820.
21. Gubbiotti MA, Neill T, Iozzo RV. A current view of perlecan in physiology and pathology: a mosaic of functions. *Matrix Biol*. 2017;57-58:285–298.
22. Yurchenco PD, Patton BL. Developmental and pathogenic mechanisms of basement membrane assembly. *Curr Pharm Des*. 2009;15:1277–1294.
23. Patel TR, Bernards C, Meier M, et al. Structural elucidation of full-length nidogen and the laminin-nidogen complex in solution. *Matrix Biol*. 2014;33:60–67.
24. Kohfeldt E, Sasaki T, Gohring W, Timpl R. Nidogen-2: a new basement membrane protein with diverse binding properties. *J Mol Biol*. 1998;282:99–109.
25. Wilson SE, Mohan RR, Mohan RR, Ambrosio R Jr, Hong J, Lee J. The corneal wound healing response: cytokine-mediated interaction of the epithelium, stroma, and inflammatory cells. *Prog Retin Eye Res*. 2001;20:625–637.
26. Wilson SE, He YG, Weng J, Zieske JD, Jester JV, Schultz GS. Effect of epidermal growth factor, hepatocyte growth factor, and keratinocyte growth factor, on proliferation, motility and differentiation of human corneal epithelial cells. *Exp Eye Res*. 1994;59:665–678.
27. Jester JV, Huang J, Petroll WM, Cavanagh HD. TGFbeta induced myofibroblast differentiation of rabbit keratocytes requires synergistic TGF beta, PDGF and integrin signaling. *Exp Eye Res*. 2002;75:645–657.
28. Masur SK, Dewal HS, Dinh TT, Erenburg I, Petridou S. Myofibroblasts differentiate from fibroblasts when plated at low density. *Proc Natl Acad Sci U S A*. 1996;93:4219–4223.
29. Mohan RR, Hutcheon AE, Choi R, et al. Apoptosis, necrosis, proliferation, and myofibroblast generation in the stroma following LASIK and PRK. *Exp Eye Res*. 2003;76:71–87.
30. Kaur H, Chaurasia SS, Agrawal V, Suto C, Wilson SE. Corneal myofibroblast viability: opposing effects of IL-1 and TGF beta1. *Exp Eye Res*. 2009;89:152–158.
31. Hong JW, Liu JJ, Lee JS, et al. Proinflammatory chemokine induction in keratocytes and inflammatory cell infiltration into the cornea. *Invest Ophthalmol Vis Sci*. 2001;42:2795–2803.
32. Girard MT, Matsubara M, Fini ME. Transforming growth factor-beta and interleukin-1 modulate metalloproteinase expression by corneal stromal cells. *Invest Ophthalmol Vis Sci*. 1991;32:2441–2454.
33. West-Mays JA, Sadow PM, Tobin TW, Strissel KJ, Cintron C, Fini ME. Repair phenotype in corneal fibroblasts is controlled by an interleukin-1 alpha autocrine feedback loop. *Invest Ophthalmol Vis Sci*. 1997;38:1367–1379.
34. Li DQ, Lokeshwar BL, Solomon A, Monroy D, Ji Z, Pflugfelder SC. Regulation of MMP-9 production by human corneal epithelial cells. *Exp Eye Res*. 2001;73:449–459.
35. Fini ME, Strissel KJ, Girard MT, Mays JW, Rinehart WB. Interleukin 1 alpha mediates collagenase synthesis stimulated by phorbol 12-myristate 13-acetate. *J Biol Chem*. 1994;269:11291–11298.
36. Kim WJ, Mohan RR, Mohan RR, Wilson SE. Effect of PDGF, IL-1alpha, and BMP2/4 on corneal fibroblast chemotaxis: expression of the platelet-derived growth factor system in the cornea. *Invest Ophthalmol Vis Sci*. 1999;40:1364–1372.
37. Wang YZ, Zhang P, Rice AB, Bonner JC. Regulation of interleukin-1beta -induced platelet-derived growth factor receptor-alpha expression in rat pulmonary myofibroblasts by p38 mitogen-activated protein kinase. *J Biol Chem*. 2000;275:22550–22557.
38. Le M, Naridze R, Morrison J, et al. Transforming growth factor Beta 3 is required for excisional wound repair in vivo. *PLoS One*. 2012;7:e48040.
39. Fantes FE, Hanna KD, Waring GO III, Pouliquen Y, Thompson KP, Savoldelli M. Wound healing after excimer laser keratomileusis (photorefractive keratectomy) in monkeys. *Arch Ophthalmol* 1990;108:665–675.
40. Torricelli AA, Singh V, Agrawal V, Santhiago MR, Wilson SE. Transmission electron microscopy analysis of epithelial basement membrane repair in rabbit corneas with haze. *Invest Ophthalmol Vis Sci*. 2013;54:4026–4033.
41. Lassance L, Marino GK, Medeiros CS, Thangavadivel S, Wilson SE. Fibrocyte migration, differentiation and apoptosis during the corneal wound healing response to injury. *Exp Eye Res*. 2018;170:177–187.
42. Ichimaru Y, Krimmer DI, Burgess JK, Black JL, Oliver BG. TGF-beta enhances deposition of perlecan from COPD airway smooth muscle. *Am J Physiol Lung Cell Mol Physiol*. 2012;302:L325–L333.
43. Warren CR, Grindel BJ, Francis L, Carson DD, Farach-Carson MC. Transcriptional activation by NFkappaB increases perlecan/HSPG2 expression in the desmoplastic prostate tumor microenvironment. *J Cell Biochem*. 2014;115:1322–1333.
44. Carlson EC, Liu CY, Chikama T, et al. Keratocan, a cornea-specific keratan sulfate proteoglycan, is regulated by lumican. *J Biol Chem*. 2005;280:25541–25547.
45. Singh V, Santhiago MR, Barbosa FL, et al. Effect of TGF beta and PDGF-B blockade on corneal myofibroblast development in mice. *Exp Eye Res*. 2011;93:810–817.

Investigative Ophthalmology & Visual Science